# Investigation of Nonlinear Motion Experienced on a Slender-Wing Research Aircraft

A. JEAN ROSS*
*Royal Aircraft Establishment, Farnborough, Hampshire, England*

**A combined experimental and theoretical study is described of the nature of the nonlinear lateral oscillation experienced by a slender-wing aircraft at high angles of attack. Flight tests of the Handley Page 115 research aircraft confirmed the expectation that the Dutch roll oscillation is undamped at high angles of attack, and also showed that a limit cycle develops, with steady amplitude in bank angle of about 30°. The measured stability derivatives are given, together with the responses obtained from the RAE flight dynamics simulator, in which the digital computation of the equations of motion uses the static aerodynamic data directly from a controlled model in a wind tunnel. The motion is also analysed theoretically using a new approximate method for obtaining solutions for nonlinear differential equations. The analysis gives the conditions sufficient for the existence of a sustained oscillation, and its amplitude and frequency in terms of the aerodynamic and inertia properties of the aircraft.**

## Nomenclature

$a_{2n+1},b_{2n+1},c_{2n+1},d_{2n+1}$ = coefficients of terms in nonlinear differential Eq. (2)
$C_l$ = rolling moment/$(\rho V^2 Ss)$
$C_n$ = yawing moment/$(\rho V^2 Ss)$
$C_Y$ = sideforce/$(\frac{1}{2}\rho V^2 S)$
$e_x,e_z$ = $-I_{xz}/I_x$, $-I_{xz}/I_z$, respectively
$g_1,g_2$ = gravity components along body axes
$I_{xz}$ = product of inertia about geometric body axes, kg m²
$I_x$ = moment of inertia in roll, kg m²
$i_x$ = $I_x/ms^2$
$I_z$ = moment of inertia in yaw, kg m²
$i_z$ = $I_z/ms^2$
$l_1,l_3 \ldots$ = coefficients in expansion of $C_l(\beta)$ $= \sum_{n=0}^{N} l_{2n+1}\beta^{2n+1}$
$l_p$ = $\partial C_l/\partial(ps/V)$
$l_r$ = $\partial C_l/\partial(rs/V)$
$l_v$ = $\partial C_l/\partial\beta$
$m$ = mass of aircraft, kg
$n_1,n_3 \ldots$ = coefficients in expansion of $C_n(\beta)$ $= \sum_{n=0}^{N} n_{2n+1}\beta^{2n+1}$
$n_p$ = $\partial C_n/\partial(ps/V)$
$n_r$ = $\partial C_n/\partial(rs/V)$
$n_v$ = $\partial C_n/\partial\beta$
$p$ = rate of roll, rad/sec
$r$ = rate of yaw, rad/sec
$R(\sigma)$ = modified Routh's discriminant
$s$ = semispan of wing, m
$S$ = area of wing, m²
$t$ = time, sec
$v$ = sideslip velocity, m/sec
$V$ = velocity of aircraft, m/sec
$y_1,y_3 \ldots$ = coefficients in expansion of $\frac{1}{2}C_Y$ $= \sum_{n=0}^{N} y_{2n+1}\beta^{2n+1}$
$y_p$ = $\frac{1}{2}\partial C_Y/\partial(ps/V)$
$y_r$ = $\frac{1}{2}\partial C_Y/\partial(rs/V)$
$y_v$ = $\frac{1}{2}\partial C_Y/\partial\beta$
$\alpha$ = angle of attack
$\beta$ = angle of sideslip, rad; $\beta = \sigma\cos\phi$
$\lambda$ = nonlinear damping factor, $\lambda = \dot{\sigma}/\sigma$
$\rho$ = air density, kg/m³
$\sigma$ = amplitude of oscillation in $\beta$
$\varphi$ = angle of bank
$\phi$ = nonlinear phase angle
$\psi$ = angle of yaw
$\omega$ = nonlinear frequency, $\omega = \dot{\phi}$

Presented as Paper 72-62 at the AIAA 10th Aerospace Sciences Meeting, San Diego, Calif., January 17–19, 1972; submitted February 3, 1972; revision received June 13, 1972. Acknowledgment is due to the late L. J. Beecham, of the Royal Aircraft Establishment, who inspired both of the new techniques described in this paper. British Crown Copyright, reproduced with the permission of the Controller, Her Britannic Majesty's Stationery Office.

Index category: Aircraft Handling, Stability, and Control.

* Principal Scientific Officer, Aerodynamics Department.

## Introduction

THE Dutch roll characteristics of slender-wing aircraft have been of special interest throughout the development of a design for a supersonic airliner. Early experiments with models showed that the oscillation can be unstable, in the sense of being undamped, at high angles of attack close to those which may be required for landing. This loss in damping could be attributed to low damping-in-roll, large yaw/roll inertia ratio, and large rolling moment due to sideslip, the latter affecting the distribution of total damping between the lateral modes. In order to assess the possible handling difficulties, it was decided to build a small research aircraft, the Handley Page 115, which first flew in 1961. Contrary to expectation, the handling qualities did not present any serious problems.[1] In particular, the Dutch roll oscillation did not diverge completely at large angles of attack, but exhibited a limit cycle type of motion, with a constant amplitude in angle of bank of 30° or so.

To examine this phenomenon, a simple model was made for testing in a new facility at the Royal Aircraft Establishment, the flight dynamic wind-tunnel simulator,[2] specially developed to study dynamic effects of nonlinear aerodynamics.[3] The static wind-tunnel tests indicated that the sideforce and moments due to sideslip are nonlinear with sideslip and with angle of attack.[4] In the flight dynamics simulator, the forces and moments due to angles of attack and sideslip are measured in the wind tunnel, processed on-line, and used directly as data in the digital computation of the equations of motion. The forces and moments due to rates of pitch, roll and yaw are stored in the computer as functions of angles of attack, the values being obtained from experiments using the oscillatory rig.[5] The resulting attitude of the aircraft relative to wind is calculated, and servo-control of the model

in the tunnel allows it to be moved accordingly, the time-scale of the computation being chosen so that the rotations are sufficiently slow not to contribute to the measured forces and moments.

The responses obtained in the simulation were characteristic of the aircraft response. The Dutch roll oscillation was stable at low angles of attack, and diverged to a sustained oscillation at high angles of attack. It was observed that the mean angle of attack in the sustained oscillation was sensibly constant, with a small-amplitude oscillation of twice the lateral frequency, so that it seemed possible to treat the motion as purely lateral in a theoretical study.

For this study, a new approximate method was used, to obtain approximate analytic solutions of the nonlinear differential equations.[6] The method is an extension of the classical work of Kryloff and Bogoliuboff,[7] developed for the study of oscillatory systems. Their concept of averaging over one cycle is retained, but an improved approximation is introduced. The analysis gives the conditions sufficient for the existence of a sustained oscillation, and its amplitude and frequency, in terms of the aerodynamic and inertia properties of the aircraft.[8]

The approximate values of frequency and amplitude, and of the variation of damping with amplitude in the transient oscillation, are shown to be in excellent agreement with results from exact digital computer solutions. Comparisons with the responses obtained in the flight dynamic simulator also show good agreement for frequency, and the character of the variation of the amplitude with mean angle of attack is predicted satisfactorily, although its magnitude is overestimated.

This combined experimental and theoretical approach has given an insight to the mechanism of a new type of aircraft response, so that it is now possible to identify effects of the nonlinear aerodynamic forces and moments, to quantify them, and to relate them to the nature of the nonlinearities.

## Description of Aircraft

The Handley Page 115 research aircraft (Fig. 1) was built specifically to investigate the aerodynamic characteristics and handling qualities of slender-wing designs at low-speed flight conditions. The wing has a delta-like planform with leading-edge sweep of 75°, and the streamwise tips are such that the span/centerline-chord ratio is 0.5 (aspect ratio = 0.925). The wing section is symmetrical, biconvex and 6% thick, with effectively sharp leading and trailing edges, and the full-span elevons have a constant chord. The fin has leading-edge sweep of 60° and taper ratio 0.535. The rudder and elevon controls are manually operated. Because the engine is mounted above the upper surface of the wing, and the cockpit mainly below the wing, the principal inertia axis is significantly nose-down relative to the fuselage datum. The yaw/roll inertia ratio is large, being about 12.

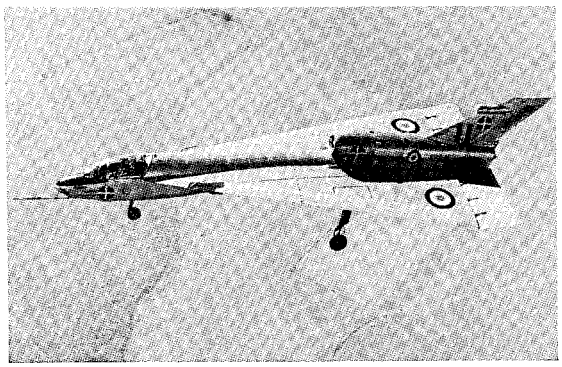

Fig. 1 The HP 115 aircraft.

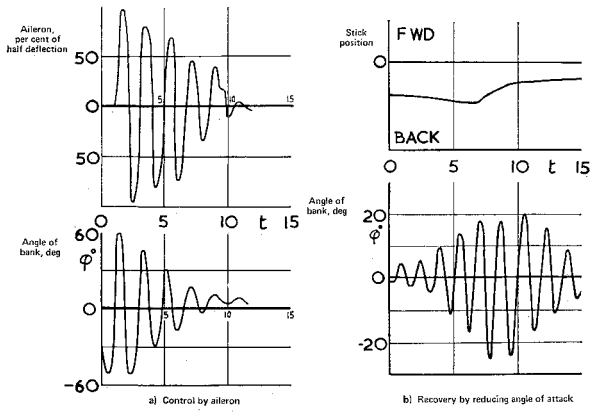


Fig. 2 Flight records at high angle of attack.

The behavior in Dutch roll has been of particular interest throughout the flight tests, which began in 1961. Prior to the first flights the aerodynamic derivatives had been estimated, so that the lateral stability characteristics could be predicted. As expected, the lateral oscillation becomes undamped as the angle of attack increases, zero damping occurring in flight at about $C_L \approx 0.55$, $\alpha \approx 19°$. It was found that flight at angles of attack greater than 19° is controllable, the oscillation diverging gently to a sustained oscillation in bank, of constant amplitude. At $\alpha \approx 21°$, with controls fixed, the amplitude is about $\pm 30°$, and at $\alpha \approx 30°$ the amplitude is increased to $\pm 40°$, with an oscillation of some $\pm 3°$ in associated yaw. This mode of motion, which has a frequency of about 0.4 Hz, can be suppressed by instinctive and easy use of conventional roll inputs, keeping the angle of attack constant, and is damped out if angle of attack is reduced via pitch control.[9] The ease with which the pilots have controlled this unusual type of response (Fig. 2) seems to be due mainly to the precise and powerful ailerons. In addition, the airflow over the wing remains well-behaved, so that the aerodynamic forces and moments do not change suddenly as angle of attack increases.

Conventional test techniques have been used to determine the lateral aerodynamic stability and control derivatives,[1] and the results will be discussed briefly in the following section. The sideslip derivatives were obtained from steady sideslip tests, and also from analysis of the Dutch-roll responses by the time-vector method. The latter also gives the damping derivatives due to rates of roll and yaw. The divergent oscillations could also be analyzed for small amplitudes, to give the lateral derivatives at the high angles of attack. Of course, some nonlinear characteristics must cause the limit cycle type of response, and these are not accounted for in the usual representation of the aerodynamics by derivatives.

## Wind-Tunnel Tests

Extensive low-speed tunnel tests have been made of the HP 115 to give the necessary background to the flight experiments. An eighth-scale model was tested in the RAE 13ft × 9ft low-speed tunnel, in parallel with the flight test program, so that the sideslip and control derivatives could be compared.[4] Later, the oscillatory rig at RAE Bedford was used, again with an eighth-scale model, to measure the derivatives due to rates of roll and yaw, and to obtain the sideslip derivatives in oscillatory conditions.[5,10]

The control derivatives measured in the static tunnel tests agreed reasonably well with the flight results, and are not discussed further. The sideforce and moments due to sideslip showed significant nonlinearities in their variation with sideslip, particularly the yawing moment $C_n$, but slopes taken

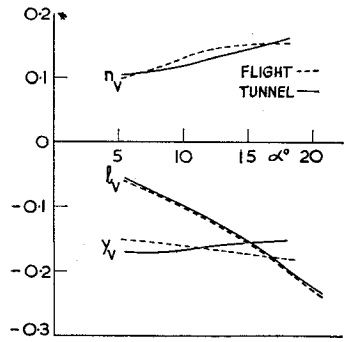


Fig. 3 Derivatives due to sideslip.

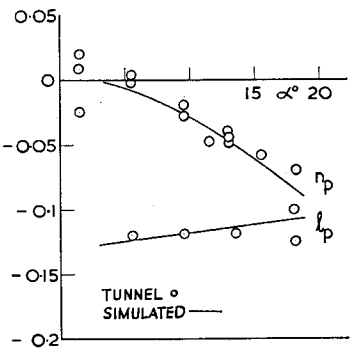


Fig. 4 Derivatives due to rate of roll.

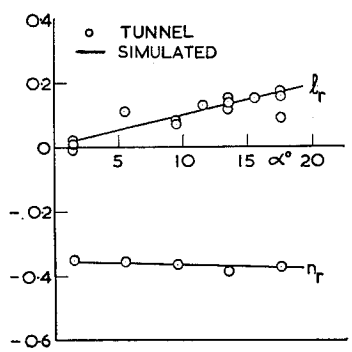


Fig. 5 Derivatives due to rate of yaw.

through an appropriate range of $\beta$ (0°–5°) give good agreement with the derivatives obtained from the steady sideslip tests in flight (Fig. 3). The oscillatory measurements of the sideslip derivatives, through small amplitude, are also in reasonable agreement.

The wind-tunnel results for the derivatives due to rates of roll and yaw are shown in Figs. 4 and 5. The values of $l_p$ and $n_r$ obtained from the flight tests are close to those used in the simulation of the full-scale motion in a wind tunnel, for which the variation of these derivatives with angle of attack is represented by simple polynomials (Table 1).

## Simulation in the Wind Tunnel

Since the static tunnel tests indicated that the sideforce and rolling and yawing moments due to sideslip are markedly nonlinear with sideslip, it was decided to use the wind-tunnel flight dynamics simulator to see if the flight behavior could be reproduced. The simulator was originally designed to investigate the response of vehicles, at supersonic Mach number, for which the static aerodynamics predominate.[2] The wind-tunnel supplies these static forces and moments to an on-line computer, which solves the equations of motion for the full-scale vehicle. Data on inertia characteristics and the derivatives due to angular rates are supplied to the computer in a conventional manner. The model is then rotated

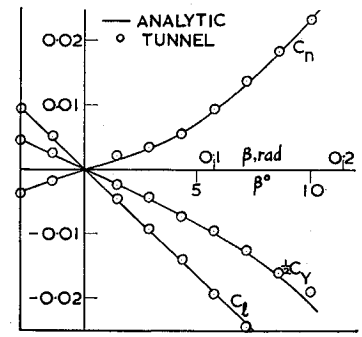


Fig. 6 Sideforce and moments due to sideslip, $\alpha = 14.3°$.

to the computed attitude relative to wind, so that the simulation proceeds (at an extended time-scale) and the responses can be recorded continuously. The facility is installed in the RAE 18in. × 18in. supersonic wind tunnel, which was modified to give subsonic flow in the working section by installing a choked second throat downstream of the working section. The model of the HP 115 tested was $\frac{1}{40}$ scale, with double-wedge sections for both wing and fin to aid manufacture, as the experiments were aimed at obtaining qualitative results, rather than precise measurements.

The full six degrees of freedom were represented in the computer, so that the wind tunnel supplied lift, drag, pitching moment, sideforce, rolling moment and yawing moment at combined angle of attack and sideslip (Fig. 6). These are slightly different in magnitude to those measured on the larger-scale, more-representative model, but the discrepancies do not affect the character of the responses. The aerodynamic derivatives due to rates of pitch, roll and yaw were computed from the polynomials in angle of attack, fitted to the experimental results. The inertia data, and formulas for the lateral rotary derivatives, are given in Table 1.

The responses obtained in the wind-tunnel simulator display all the features experienced in flight. At low angles of attack, a yawing moment had to be applied to start the motion, which then decayed quite quickly (Fig. 7a). The lateral response does not appear to be affected by the small changes in angle of attack, $\alpha$, the latter being due to the cross-coupling between the longitudinal and lateral modes. As the trimmed angle of attack is increased, the damping of the oscillation decreases, so that a neutrally stable state is

**Table 1 Numerical values of parameters**

| Inertias, etc. | | Aerodynamic derivatives |
|---|---|---|
| $m$ | 2,154 kg | $y_p = 0.014 + 0.505\alpha - 0.47\alpha^2$ |
| $I_{xx}$ | 2,182 kg m$^2$ | $l_p = -0.132 + 0.08\alpha$ |
| $I_{zz}$ | 25,430 kg m$^2$ | $n_p = 0.0125\alpha - 0.938\alpha^2$ |
| $I_{xz}$ | 1,615 kg m$^2$ | $y_r = 0$ |
| $S$ | 40.18 m$^2$ | $l_r = 0.006 + 0.54\alpha$ |
| $s$ | 3.05 m | $n_r = -0.351 - 0.089\alpha$ |

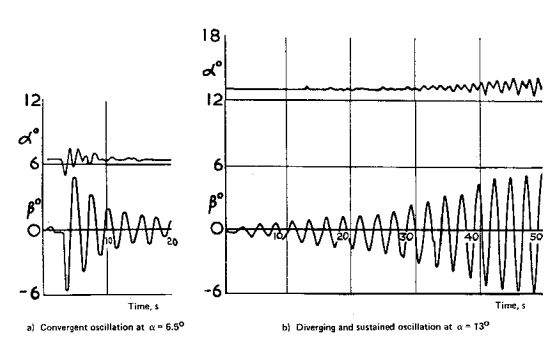


Fig. 7 Simulated responses at $\alpha = 6.5°$ and 13°.

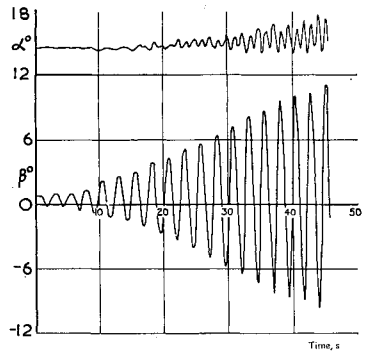


Fig. 8 Simulated responses at $\alpha = 14.5°$.

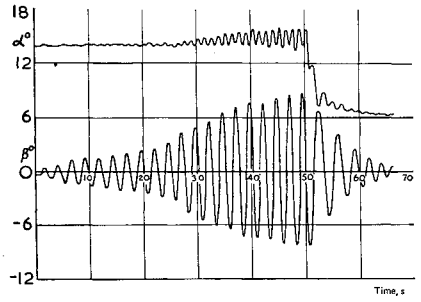


Fig. 9 Simulated recovery by reducing $\alpha_{trim}$.

reached.† Above the angle of attack at which this occurs, it is not necessary to give the aircraft model a disturbance, as the initially divergent oscillation is excited by any small random disturbance, but the rate of divergence decreases as the amplitude increases, until a steady value of amplitude is reached (Fig. 7b). The results show that the amplitude of the sustained oscillation increases as the angle of attack is increased, and for some of the large values of $\alpha_{trim}$ the amplitude is still increasing at the end of the record (Fig. 8). A simulation of a recovery was also made, and clearly shows the decay of the oscillation as the angle of attack is reduced to a new trimmed value (Fig. 9).

## Theoretical Analysis

A new method of obtaining approximate analytic solutions to second-order nonlinear differential equations has proved to be applicable to a wide variety of problems with oscillatory characteristics,[6] and the extension to fourth-order equations has been made for the present problem. The model in the simulator was free to respond longitudinally, but the resulting change in angle of attack was regarded as sufficiently small for the longitudinal equations of motion to be neglected in the basic theoretical treatment.

The lateral equations of motion of an aircraft, flying at a given speed (or angle of attack) are usually expressed in terms of perturbations in sideslip velocity, roll rate and yaw rate, with aerodynamic forces and moments approximated by their first derivatives with respect to the perturbations. For given angle of attack, the forces and moments due to roll rate and yaw were represented in this manner in the simulation, but the sideforce and moments due to sideslip velocity were measured directly. The static measurements could, however, be represented in the equations by polynomials in sideslip angle, ($\beta$ in radians) so that the equations of motion may be written as:

$$V\frac{d\beta}{dt} - V\alpha p + Vr - g_1\varphi + g_2\psi = \frac{\rho SV^2}{m}\left[y_1\beta + y_3\beta^3 + \cdots + y_p\frac{ps}{V} + y_r\frac{rs}{V}\right] \quad (1a)$$

$$\frac{dp}{dt} - \frac{I_{xz}}{I_x}\frac{dr}{dt} = \frac{\rho SV^2 s}{I_x}\left[l_1\beta + l_3\beta^3 + \cdots + l_p\frac{ps}{V} + l_r\frac{rs}{V}\right] \quad (1b)$$

$$\frac{dr}{dt} - \frac{I_{xz}}{I_z}\frac{dp}{dt} = \frac{\rho SV^2 s}{I_z}\left[n_1\beta + n_3\beta^3 + \cdots + n_p\frac{ps}{V} + n_r\frac{rs}{V}\right] \quad (1c)$$

$$(d\varphi/dt) - p = 0 \quad (1d)$$

$$(d\psi/dt) - r = 0 \quad (1e)$$

These simultaneous differential equations reduce to a fourth-order equation in $\beta$,

$$\frac{d^4\beta}{dt^4} + \frac{d^3A(\beta)}{dt^3} + \frac{d^2B(\beta)}{dt^2} + \frac{dC(\beta)}{dt} + D(\beta) = 0 \quad (2)$$

where $A(\beta) \cdots D(\beta)$ are polynomials in odd powers of $\beta$,

$$A(\beta) = a_1\beta + a_3\beta^3 + \cdots \text{ etc.} \quad (3)$$

The coefficients $a_1, b_1, c_1, d_1$ are the usual combination of derivatives obtained in the linear stability analysis, e.g.,

$$-a_1 = \frac{\rho SV}{m}\left[y_1 + \left\{\frac{l_p}{i_x} + \frac{n_r}{i_z} - \frac{e_x n_p}{i_z} - \frac{e_z l_r}{i_x}\right\}\Big/\{1 - e_x e_z\}\right]$$

The nonlinear terms are obtained by inspection, replacing $y_1$ by $y_3$ etc. in $a_1 \cdots d_1$, e.g.,

$$-a_3 = y_3/(\rho SV/m)$$

with no contributions from $l_3$ and $n_3$ in $a_3$.

The technique used to analyze Eq. (2) is to assume that the oscillatory mode in the response can be represented‡ as a product of an amplitude $\sigma$ and a sinusoidal function, that is

$$\beta = \sigma\cos\phi \quad (4)$$

The frequency $\omega$ and damping $\lambda$ are defined as

$$\omega = \dot{\phi} \qquad \lambda = \dot{\sigma}/\sigma \quad (5)$$

and are taken to be functions of the amplitude $\sigma$. The assumption is made that $\omega$ and $\lambda$ do not vary greatly in one cycle of the oscillation. Equation (2) may then be written as

$$\frac{d^4\beta}{dt^4} \approx \sigma[(\lambda^4 - 6\lambda^2\omega^2 + \omega^4)\cos\phi + 4\omega(\omega^2 - \lambda^2)\sin\phi]$$

$$= \sigma F(\lambda,\omega,\sigma,\cos\phi,\sin\phi) + \left(\text{terms in } \frac{d\omega}{d\sigma}, \frac{d\lambda}{d\sigma}\right)$$

As in the Kryloff and Bogoliuboff method, this equation is solved by taking average values over one cycle, so that the terms in $d\omega/d\sigma$ and $d\lambda/d\sigma$ are neglected in the first approximation; $\omega$ and $\lambda$ are interpreted as having values at a particular $\sigma$ within the cycle, assumed here to be at midcycle.[7] Two equations result

$$\lambda^4 - 6\lambda^2\omega^2 + \omega^4 = \frac{1}{\pi}\int_0^{2\pi} F\cos\phi d\phi$$

$$= -\sum_{n=0}^{N}\sigma^{2n}X(n)[a_{2n+1}(2n+1)\lambda\{\lambda^2(2n+1)^2 - 3\omega^2\} +$$

$$b_{2n+1}\{\lambda^2(2n+1)^2 - \omega^2\} + c_{2n+1}(2n+1)\lambda + d_{2n+1}] \quad (6)$$

† In the simulation, this occurred at a lower angle of attack (about 11°) than in flight (about 19°). This is probably due to a scaling error in the computer, such that $\frac{1}{2}C_Y$ was used inadvertently as input to the sideforce equation instead of $C_Y$ (see "Discussion of Results").

‡ The more general expression analogous to the modes present in the linearized system, $\beta = \sigma_1\cos\phi + \sigma_2 + \sigma_3$, has also been studied, and it can be shown that the sum of the exponential type modes, $\sigma_2 + \sigma_3$, is zero in the limit cycle.[8]

and

$$4\omega(\omega^2 - \lambda^2) = \frac{1}{\pi}\int_0^{2\pi} F \sin\phi d\phi$$

$$= \sum_{n=0}^{N} \sigma^{2n} X(n)[a_{2n+1}\{3\lambda^2(2n+1)^2 - \omega^2\} + 2b_{2n+1}(2n+1) + c_{2n+1}] \quad (7)$$

where

$$X(n) = [(2n+1)!]/[2^{2n}n!(n+1)!] \quad (8)$$

These equations may be combined in a similar way to the familiar linear complex roots treatment [where $\beta = C\exp(\lambda + i\omega)t$], to give

$$(\lambda + i\omega)^4 + \sum_{n=0}^{N} \sigma^{2n} X(n)[a_{2n+1}\{\lambda + 2n\lambda + i\omega\}^3 + b_{2n+1}\{\lambda + 2n\lambda + i\omega\}^2 + c_{2n+1}\{\lambda + 2n\lambda + i\omega\} + d_{2n+1}] = 0 \quad (9)$$

For small amplitudes, the higher-order terms in $\sigma$ may be neglected and the equations give the frequency and damping of the Dutch roll oscillation for the linearized lateral equations of motion. In the limit cycle $\lambda = 0$, and elimination of $\omega$ between Eq. (6) and (7) leads to the condition that an expression analogous to Routh's discriminant be zero, that is, $R(\sigma_s) = 0$ gives the amplitude $\sigma_s$ of the limit cycle, where

$$R(\sigma) = \left[\sum_{n=0}^{N} a_{2n+1}X(n)\sigma^{2n}\right]\left[\sum_{n=0}^{N} b_{2n+1}X(n)\sigma^{2n}\right] \times \left[\sum_{n=0}^{N} c_{2n+1}X(n)\sigma^{2n}\right] - \left[\sum_{n=0}^{N} c_{2n+1}X(n)\sigma^{2n}\right]^2 - \left[\sum_{n=0}^{N} d_{2n+1}X(n)\sigma^{2n}\right]\left[\sum_{n=0}^{N} a_{2n+1}X(n)\sigma^{2n}\right]^2 \quad (10)$$

The first approximation to this condition gives that

$$\sigma_s^2 \approx -R(0)/[\partial R/\partial\sigma^2]_{\sigma=0} \quad (11)$$

so that a limit cycle exists, ($\sigma_s$ is real), when $R(0)$ and $\partial R/\partial\sigma^2$ are of opposite sign.

The frequency in the limit cycle is given by

$$\omega_s^2 = \left[\sum_{n=0}^{N} c_{2n+1}X(n)\sigma_s^{2n}\right] \Big/ \left[\sum_{n=0}^{N} a_{2n+1}X(n)\sigma_s^{2n}\right] \quad (12)$$

These approximate solutions have been compared with computed responses to the equations of motion at two angles of attack, where the nonlinearity is confined to a cubic term with $n_3 \approx 20n_1$. The amplitude and frequency of the limit cycle agree very well (Fig. 10). The variation of the damping with amplitude is also determined very closely, as shown by the envelope in Fig. 11. This has been obtained by using the relation $\dot{\sigma} = \lambda\sigma$ to give the time taken for the amplitude to grow from $\sigma_1$ to $\sigma_2$,

$$t_2 - t_1 = \int_{\sigma_1}^{\sigma_2} \frac{d\sigma}{\lambda\sigma} \quad (13)$$

The integral has to be evaluated numerically, but it was found that, for cubic nonlinearity, a good approximation to $\lambda$ is given by

$$\lambda \approx \lambda_0[1 - (\sigma/\sigma_s)^2] \quad (14)$$

where $\lambda_0$ is the damping of the Dutch roll oscillation, obtained from the linearized equations of motion.

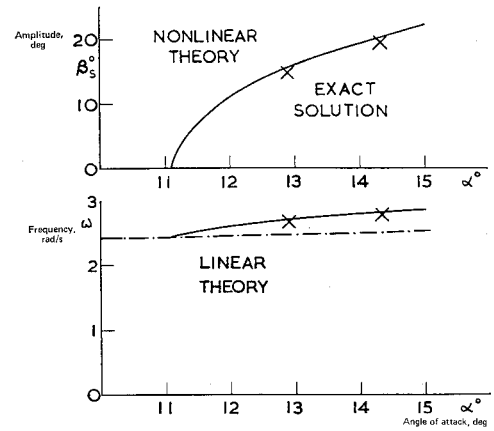


**Fig. 10 Amplitude and frequency of sustained oscillation from nonlinear theory and numerical integration.**

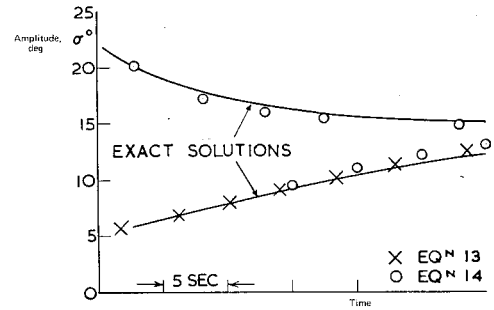


**Fig. 11 Amplitude of oscillation from nonlinear theory and numerical integration.**

**Table 2 Comparison of results**

| | Approximate | Numerical integration |
|---|---|---|
| Amplitude in roll | 2.5 rad/sec | 2.5 rad/sec |
| Amplitude in yaw | 0.11 rad/sec | 0.12 rad/sec |
| Phase of roll | −68.7° | −69° |
| Phase of yaw | 47.2° | 42° |

The computed responses also indicated that the sustained oscillation is a true limit cycle, in that an initial disturbance greater in magnitude than the steady value converged to the steady value. Analytic expressions for the amplitudes and phases of $p$, $r$, and so $\varphi$, $\psi$, in the limit cycle have been obtained. The results are again very close to the computed solution, a comparison being given for one example in Table 2, for $\alpha = 12.9°$.

## Discussion of Results

### Dutch Roll Characteristics

The flight and simulated responses have been analysed on a linear basis, when the amplitudes are small, to give frequency and damping of the Dutch roll oscillations. The frequency agrees well, and there is only small variation with angle of attack (Fig. 12). However, the damping of the simulated responses is smaller than the flight values, so that the oscillation becomes divergent at a lower angle of attack than in flight. Linear theory has been used to obtain values of the damping for flight and simulation, and good correlation for the latter is obtained if $\frac{1}{2}y_v$ is used instead of $y_v$. (The larger values of lift and rolling moment due to sideslip

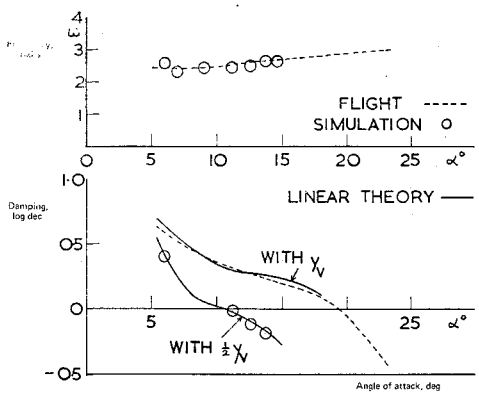


**Fig. 12 Frequency and damping of Dutch roll oscillation at small amplitudes.**

obtained in the simple tunnel model were also used for the calculation of the simulator values.) Unfortunately there is now no means of checking this further, but it does seem likely that an error occurred in the scaling of the computer. However, the main characteristics of the full-scale motion were simulated so well that it has not been thought necessary to repeat the experiments. The numerical value of $\frac{1}{2}y_v$ has been used for $y_1$ in the nonlinear theoretical calculations.

### Sustained Oscillation

The frequency of the divergent oscillations at large amplitudes, obtained in the simulation, agrees well with the theoretical values obtained from Eq. (12), using polynomials of degree 3 (i.e., linear and cubic terms) to represent $C_n$ and $C_Y$, and linear $C_l$.

A detailed examination of the apparently steady amplitude oscillation obtained in the simulation showed that the amplitude was still increasing slightly because of the finite duration of the tunnel tests. Before comparing the steady-state amplitudes with the theoretical predictions it was therefore necessary to extrapolate the measured values to the true terminal values. This was achieved by determining the point of inflection of the experimental amplitude envelope of sideslip angle, and using the approximation of Eq. (14) to relate the amplitude $\sigma_i$ to the steady amplitude $\sigma_s$ to give

$$\sigma_s = (3)^{1/2}\sigma_i$$

The experimental results, corrected in this manner are compared with approximate theory in Fig. 13. The theory overestimates the experimental values, but the trend with increasing angle of attack is the same. The theoretical value of $\sigma_s$ was found to be dependent on the exact form of the polynomials chosen for $C_n(\beta)$ and $C_Y(\beta)$, and including a quintic term in $C_n(\beta)$ did improve the agreement for $\sigma_s$, but did not give such a good fit to the $C_n(\beta)$ data. It was not thought worthwhile to attempt to find higher order polynomials to achieve closer agreement.

The comparison with the flight results can only be qualitative, but it is encouraging to note that the simulated and calculated angles of bank in the sustained oscillation, at an angle of attack 2° above that for divergence, are both about 30°, as in flight.

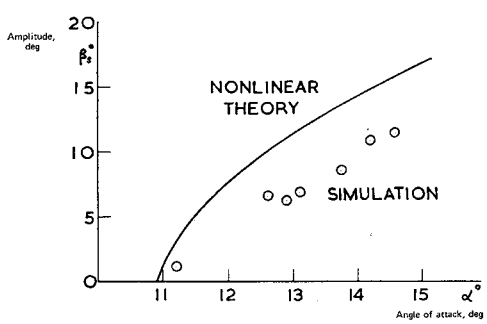


**Fig. 13 Amplitude of sustained oscillation from nonlinear theory and simulated responses.**

### Interpretation of Nonlinear Characteristics

The analysis has been given for general nonlinear $C_Y$, $C_l$ and $C_n$, but the main characteristics of the nonlinear response are obtained by considering only one additional term to the linearized equations, a cubic term in $C_n(\beta)$. This is a reasonable representation of the sideslip data. Equations (6) and (7) then simplify to give

$$\sigma_s^2 \approx \frac{4}{3}\frac{[c_1^2 - a_1b_1c_1 + a_1^2d_1]}{[a_1b_1c_3 + a_1b_3c_1 - a_1^2d_3 - 2c_1c_3]} \tag{15}$$

$$\omega_s^2 = [c_1 + \tfrac{3}{4}c_3\sigma_s^2]/a_1 \tag{16}$$

The numerator of Eq. (15) is proportional to Routh's discriminant, $R(0)$, of the stability polynomial evaluated as if the nonlinearities were absent. For the HP 115 model, $R(0)$ is zero at $\alpha = 11°$ so that for $\alpha < 11°$, a normal convergent oscillation can be expected, and for $\alpha > 11°$, a divergent oscillation will occur. This will tend to a sustained oscillation if the denominator and numerator of Eq. (15) are of the same sign, to give real $\sigma_s$. The denominator is proportional to $n_3$, the cubic coefficient in $C_n(\beta)$, and it is found that $n_3$ has to be positive for $\sigma_s$ to exist, that is, the varying $\partial C_n/\partial\beta$ has to be increasing with increasing angle of sideslip. The amplitude of the sustained oscillation is highly dependent on the magnitude of the nonlinearity, since $\sigma_s^2$ is inversely proportional to $n_3$ [Eq. (15)]. On the other hand, the frequency is independent of the magnitude of $n_3$, the nonlinear term in Eq. (16) being proportional to the product $n_3\sigma_s^2$. Additional nonlinearities, either extra terms in $C_n(\beta)$, or nonlinear contributions to $C_Y(\beta)$ and $C_l(\beta)$ affect the magnitudes of $\sigma_s$ and $\omega_s$, according to the more complicated relations given in Eqs. (11) and (12).

## Concluding Remarks

This study of the nonlinear lateral oscillation experienced by the HP 115 aircraft in flight has successfully demonstrated the use of the two new techniques, experimentally, that of obtaining data direct from a wind tunnel for the computation of simulated full-scale responses, and theoretically, that of deriving approximate analytic solutions to nonlinear differential equations. The combined results lead to a good understanding of the relation between the nonlinear aerodynamic forces and moments and the dynamic response. A nonlinear yawing moment due to sideslip, with increasing slope as angle of sideslip increases, is sufficient to cause an initially divergent Dutch roll oscillation to become a limit cycle. Additional nonlinearity in sideforce due to sideslip affects the amplitude of the sustained oscillation, with only small effect on the frequency. The theoretical values of the frequency and amplitude of the sustained oscillation are in satisfactory agreement with the simulated responses, which themselves have similar characteristics to the flight results.

## References

[1] Bisgood, P. L., "Results of Flight Tests on a Slender-Wing Low-Speed Research Aircraft (HP 115)," AGARD Rept. 535, 1966.

[2] Beecham, L. J., Walters, W. L., and Partridge, D. W., "Proposals for an Integrated Wind-Tunnel Flight Dynamics Simulator System," Current Paper 789, 1965, Aeronautical Research Council, London, England.

[3] Partridge, D. W. and Pecover, B. E., "An Application of the RAE Wind-Tunnel/Flight Dynamics Simulator to the Low Speed Dynamics of a Slender Delta Aircraft (HP 115)," Repts. and Memos. 3669, 1969, Aeronautical Research Council, London, England.

[4] Engler, P. B. E. and Moss, G. F., "Low-Speed Tunnel Tests on a $\frac{1}{8}$th Scale Model of the Handley Page HP 115," Repts. and Memos. 3486, 1965, Aeronautical Research Council, London, England.

[5] Thompson, J. S. and Fail, R. A., "Oscillatory Derivative Measurement on Sting-Mounted Wind-Tunnel Models at RAE Bedford," AGARD Current Paper 17, 1966.

[6] Beecham, L. J. and Titchener, I. M., "Some Notes on an Approximate Solution for the Free Oscillation Characteristics of Nonlinear Systems Typified by $\ddot{x} + F(x,\dot{x}) = 0$," Repts. and Memos. 3651, 1969, Aeronautical Research Council, London, England.

[7] Kryloff, N. and Bogoliuboff, N., *Introduction to Nonlinear Mechanics*, Princeton University Press, Princeton, N.J., 1937.

[8] Ross, A. J. and Beecham, L. J., "An Approximate Analysis of the Nonlinear Lateral Motion of a Slender Aircraft (HP 115) at Low Speeds," Repts. and Memos. 3674, 1971, Aeronautical Research Council, London, England.

[9] Henderson, J. M., "Low Speed Handling of a Slender Delta (HP 115)," *Journal of the Royal Aeronautical Society*, Vol. 69, No. 653, 1965, pp. 311–324.

[10] Thompson, J. S., Fail, R. A., and Inglesby, J. V., "Low Speed Wind-Tunnel Measurements of the Oscillatory Lateral Stability Derivatives for a Model of the Slender Aircraft (HP 115) Including the Effects of Frequency Parameter," Current Paper 1097, 1969, Aeronautical Research Council, London, England.

SEPTEMBER 1972 J. AIRCRAFT VOL. 9, NO. 9

# An Improved Solution of the Two-Dimensional Jet-Flapped Airfoil Problem

RICHARD G. LEAMON*
*Naval Ordnance Laboratory, White Oak, Md.*
AND
ALLEN PLOTKIN†
*University of Maryland, College Park, Md.*

**A method of solution is developed for a two-dimensional jet-flapped airfoil in potential flow. Numerical solutions are obtained which contain the proper singularities and which properly satisfy the boundary conditions on the airfoil and jet surfaces along their actual positions. A discussion of previous work is given. Comparisons of the method with previous work and experimental measurements are made. For momentum coefficients up to 1.0 and initial jet deflection angles of up to 60.0° the present method gives values of the sectional lift and pitching moment coefficients which differ from previous methods—those using the shallow jet approximation—by up to 16% but which lie within the range of experimental results.**

## I. Introduction

THE jet flap is a high lift device which employs a thin jet of high speed air ejected downward at the trailing edge of an airfoil (Fig. 1). The phenomenon was first extensively investigated by Hagedorn and Ruden.[1] Subsequent tests have produced sectional lift coefficients as high as 10.0. A sketch of the early development of the basic principle and accompanying theory is given in Stafford.[8] High lift coefficients are achieved by using the jet for two reasons: 1) a change in the pressure distribution over the airfoil chord which produces a net increase in the lift and 2) the reaction to the vertical momentum exhausted by the airfoil into the jet.

This paper presents a new method of calculating two-dimensional potential flow about a jet-flapped airfoil. Previous methods, accorded to Spence,[3] Hough,[4] and Malavard,[5] obtain a solution by distributing a singular solution (vortex sheet) along a semi-infinite line parallel to the undisturbed flow and passing through the trailing edge of the airfoil (Fig. 2a). Such a representation is here denoted as the shallow jet approximation. The present method places the singular solution along the mean camber line of the airfoil and the mean position of the jet (Fig. 2b) and, in contrast to these previous methods, satisfies the boundary condition at the actual position of these surfaces. This representation provides more accurate results in the sense of satisfying the boundary conditions more realistically at the cost of considerable mathematical complication. This representation was also used by Herold[6] who constructed a solution using a finite number of discrete vortex filaments placed along the airfoil and jet.

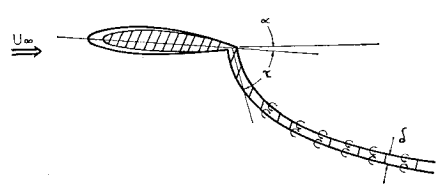


**Fig. 1 Jet-flapped airfoil at angle of attack $\alpha$ with initial jet deflection $\tau$.**

Received August 27, 1971; revision received April 17, 1972. The computer time for this research was supplied by the Computer Science Center of the University of Maryland. The authors would like to thank H. Snay, W. Melnik, and L. Filotas for their useful suggestions.

Index categories: Subsonic and Transonic Flows; Jets, Wakes, and Viscid-Inviscid Flow Interactions

* Research Physicist.

† Associate Professor of Aerospace Engineering. Member AIAA.